NASA TECHNICAL MEMORANDUM

NASA TM X-71680

NASA TM X-71680

THERMAL ANALYTIC MODEL OF A 30 CM ENGINEERING MODEL MERCURY ION THRUSTER

by Jon C. Oglebay
Lewis Research Center
Cleveland, Ohio 44135

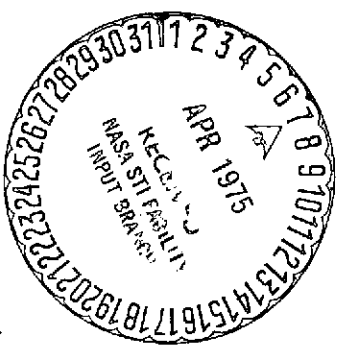

TECHNICAL PAPER to be presented at
Eleventh Electric Propulsion Conference sponsored
by American Institute of Aeronautics and Astronautics
New Orleans, Louisiana, March 19-21, 1975

THERMAL ANALYTICAL MODEL OF A 30 CM MERCURY ION THRUSTER

by Jon C. Oglebay

National Aeronautics and Space Administration
Lewis Research Center
Cleveland, Ohio 44135

ABSTRACT

A lumped parameter thermal nodal network has been developed for a 30 cm Engineering Model Mercury Ion Thruster. The network consists of approximately 100 nodes coded in SINDA format for use on the Univac 1106/1108 computer. This model takes into account internal dissipation, radiation, and conduction as well as environmental heating.

A series of tests were performed at NASA-Lewis Research Center to simulate a wide range of thermal environments on an operating 30 cm thruster, (ref. 1), instrumented to measure the temperature distribution within the thruster. The results of these tests were used to calibrate the analytical model.

Presented in this paper are a description of the analytical model along with comparisons between analytical and experimental results for the various operating conditions.

E-8262

INTRODUCTION

Missions for which the use of large ion thrusters are desired, require that the thrusters operate over a wide range of thermal environments for long periods of time (up to 5 yrs.). These missions also require having a large number of thrusters on board with as few as two or as many as nine thrusters operating at the same time. Because of the wide range of thermal environments encountered, a good analytical model is required to compute the temperature distributions within the thruster as well as predicted the thermal interaction of the thruster with the environment, adjacent thrusters and the spacecraft itself.

There have been thermal models developed for the 20 cm ion thrusters (refs. 2 and 3) as well as studies on the self-heating pattern of operating 15 and 20 cm ion thrusters (refs. 4 and 5). For these studies experimental data was obtained with operating thrusters instrumented with thermocouples located in the assumed areas of thermal dissipation. The analytical model was then adjusted to obtain agreement between the experimental and predicted temperatures.

This combined analytical/experimental approach has been used in this study. The experimental data was obtained using an operating 30 cm ion thruster (ref. 1). The analytical model was developed and the self-heating

distribution adjusted to obtain agreement with the experimentally obtained temperature distributions. This calibration procedure will be discussed.

Once the model was calibrated, it was used to study the thermal performance that could be obtained in multiple thruster operation. A comparison of the predictions of the analytical model with the data obtained in a test program (ref. 1) which simulated multiple thruster operation, will be presented.

THERMAL INVESTIGATION

Thermal Model

The concept of treating heat flow problems in terms of electrical networks has been well developed (ref. 6) and is based on the equivalence of the electrical and thermal conductance equations. The concept basically involves the determination of the thermal resistance paths within a given network and then numerically determining the resulting temperature distribution.

Based on the design configuration, a lumped mass thermal network consisting of 88 diffusion and 6 boundary nodes was constructed. The nodal layout of the thruster is shown in Figure 1. In general, the main components of the thruster (i.e., anode, engine body, ground screen, etc.) were divided into 4 equal areas circumferentially. The network allows each circumferential quadrant to see any environmental temperature desired. This capability was used to simulate multiple thruster operation.

Heat exchange within the thruster is predominately by radiation. This requires that the surface optical properties of the materials be known with a reasonable degree of accuracy. However, there can be considerable variation of the optical properties due to non-uniform surface finish, the deposition of debris from the operating thruster and any temperature dependence of the surface properties. Also, since most of the materials are metallic (i.e., low optical properties), there is the possibility of multiple reflections which complicates the computation of the radiation conductors.

Small samples of various parts of the thruster were removed and optical properties were measured experimentally between wavelengths of 1 and 15 μm. In general, the value of emissivity of the samples was between 0.10 and 0.15 at the wavelengths of interest (5 to 7 μm). A value of 0.10 was chosen as the emissivity of the thruster surfaces. However, for the interior nodes of the thruster radiating through the grids to the cold walls of the test chamber, a cavity effect emissivity of 0.50 was assumed based on data from reference 7.

The radiation exchange factor, $\mathcal{F}_{ij}$, was approximated by the following relationship developed in reference 6;

$$\mathcal{F}_{ij} = \frac{1}{\left(\frac{1}{\varepsilon_i} - 1\right) + \frac{A_i}{A_j}\left(\frac{1}{\varepsilon_j} - 1\right) + \frac{1}{F_{ij}}}$$

where ε_i and ε_j are the emissivities of the ith and jth node, A_i and A_j are the radiating areas of the ith and jth node, and F_{ij} is the geometric configuration factor between the ith and jth node. The values of F_{ij} were calculated either by hand or numerically using the computer program in reference 8.

Although radiation is the dominant means of heat transfer within the thruster, the linear conduction contribution cannot be overlooked. Therefore, it is necessary that the thermal conductivity of the materials as well as the contact resistance between joints be known. The thermal conductivities of the materials are well documented in the literature and are relatively constant over the temperature range of concern. The values for thermal conductivity used herein are presented in Table I. An experimentally obtained value of 0.0057 W/cm^2 °C was used for the joint conductance in setting up the model.

The program chosen to solve the analytical model was the Systems Improved Numerical Differencing Analyzer, or SINDA which is a thermal analyzer program described in reference 9. Once the necessary model information was obtained, it was coded in SINDA format and the steady state temperature distributions of the thruster were calculated. Predicting variations in the thermal performance of the thruster due to property changes can be done with relative ease.

Thruster Self-Heating Distribution

When the thruster is operating, heat is supplied to the various vaporizers and cathodes. These heat inputs are known and can be treated analytically without difficulty. However, there are significant heat inputs to various components of the thruster due to the ionization and acceleration processes. The distribution of this heat to the thruster is not known precisely and does present another uncertainty in a purely analytical approach.

Estimates of the self-heating distribution within operating 15 and 20 cm ion thrusters have been made by other investigators (refs. 4 and 5). The approach taken here was initially to assume that the heat distribution to the various components of the thruster was in the same ratio of the total power as finalized by Wen in (ref. 2) for a 1 amp beam current. These values were then adjusted as necessary to obtain agreement between experimental and analytical results. The same ratios were then applied for a 1.90 amp beam current and adjusted as necessary. The final values and percentage of the total dissipation to the various components for the two beam currents are shown in Table II along with the total discharge power.

In general, the final values shown in Table II are within 2 percent of those used by Wen (ref. 2). The only major difference is the amount of heat going to the engine body. Whereas Wen had approximately 9 percent of the total heat being received by the engine body, this model has approximately 25 percent. Comparing the distribution between the two beam currents shows very little difference in percentage of total heat dissipation to the various components (see Table II). Based on the above comparisons, it appears that Wen's 20 cm approximations can be used for other size thrusters.

RESULTS AND DISCUSSION

Calibration

The analytical model was calibrated using data generated at 1.9 and 1.0 amp beam currents for a single thruster in a vacuum chamber surrounded by LN_2 cold walls. These beam currents represent full power and half power respectively.

The comparison of experimental and analytical temperature distributions for these calibration tests are given in Table III. The rear shield temperatures were set at the average experimental values due to the complex nature of the support system. In general, the analytical results agree within 10° C of the experimental data for the main components of the thruster. The discrepancies in the ground screen predictions are about 20° C due principally to uncertainties in calculating view factors for a curved, perforated surfaces and difficulties in measuring accurate temperatures. The reason for the discrepancy on the main vaporizer at the 1 amp beam current is not understood at this time. Although the network does include nodes for the neutralizer assembly (Fig. 1), no comparisons between analytical and experimental results are presented. The lumped node simulation of this area is not a good representation of the actual hardware; a detailed analytical model of this area is required. However, the analysis has shown that the cathode and vaporizer of this neutralizer assembly are so isolated from the thruster that they have essentially no impact on the temperature distributions of the main components of the thruster. Therefore, the neutralizer system can be treated as an isolated body if more accurate temperature predictions for this assembly are required.

Multiple Thruster Simulation

After the model was calibrated, it was used to study the effects of multiple thruster operation. A multiple thruster array was experimentally simulated by surrounding a thruster with a variable temperature azimuthal shield similar to that shown in Figure 2. This configuration is a good simulation of a double row array of thrusters or the 2 by n array of thrusters. This shield allowed the thruster to radiate primarily to a warm body rather than the LN_2 cold walls. This would permit a thermal evaluation of an operating thruster surrounded by either operating or non-operating adjacent thrusters. The shield was instrumented with thermocouples to monitor the

shield temperatures. Strip heaters were attached uniformly to the bottom of the shield to control the temperature.

The shield was operated at two different temperatures for beam currents of 1.9 and 1.0 amps. One temperature simulated an adjacent thruster being off while the second simulated an operating adjacent thruster. For the thruster off simulation the shield was allowed to reach its equilibrium temperature without any power being supplied to it, while for the thruster operating simulation the shield was heated to 150° C.

The experimental and analytical results for the 4 multiple array simulation tests are shown in Table IV. As in the calibration tests the rear shield temperatures were set to their average experimental values. Again the analytical results agree within 10° C of the experimental values with the areas of discrepancy being the same as in the calibration tests.

Experimental temperatures on the engine body center and front increase 10 to 20° C from the calibration tests (Table III) to the intermediate shield temperature tests, but then increase only an additional 3 to 5° C when the shield is heated to 150° C. The model predicts about the same increase in temperature as the experimental data for the intermediate shield temperatures. However, when the shield is heated to 150° C, the analysis predicts a greater increase than was measured. The temperature comparisons between experimental and analytical results are also given in Figures 3 through 8.

The results of the analysis and the test program show that the main mode of heat dissipation is out the accelerator end of the thruster to the cold walls of the chamber. Limiting radiation from the engine body to the environment does not have a significant influence on the thruster temperatures.

CONCLUSIONS

An analytical thermal network for a 30 cm engineering model mercury ion thruster has been developed and calibrated against experimental data obtained from an operating 30 cm thruster.

Experimental data has been generated at both half and full beam power over a wide range of boundary temperatures. Comparisons between analytical and experimental temperatures show that the analytical model agrees within 10° C of the experimental results for the main components of the thruster.

From the results of this study, it was concluded that:

1. A realistic thermal model has been constructed to represent the thruster thermal performance with an expected accuracy of 10° C.

2. Heat losses to various components of the thruster from the plasma can be estimated with reasonable accuracy.

3. The model can be used to analyze interactions between thruster arrays, thermal environment, and the spacecraft itself.

4. The operating thruster is relatively insensitive to the boundary temperatures.

5. The main heat rejection mechanism is by radiation out the accelerator end of the thruster to the cold walls of the chamber.

REFERENCES

1. Mirtich, M. J., "The Effects of Exposure to LN_2 Temperatures and 2.5 Suns Solar Radiation on 30 Centimeter Ion Thruster Performance," TM X-71652, 1975, NASA.

2. Wen, L., Crotty, L. D. and Pawlick, E. V., "Ion Thruster Characteristics and Performance," AIAA Paper 72-476, Bethesda, Md., 1972.

3. Wen, L. and Womack, J. R., "Thruster Array Thermal Control," AIAA Paper 73-1117, Lake Tahoe, Nev., 1973.

4. Bayless, J. R., et al.: LM Cathode Thruster System. Oct. 1970, Hughes Research Labs., Malibu, Calif., JPL-952131, Jet Propulsion Lab., Pasadena, Calif.; also CR-110895, 1970, NASA.

5. Masek, T. D., "Plasma Properties and Performance of Mercury Ion Thrusters," AIAA Paper 69-256, Williamsburg, Va., 1969.

6. Kreith, F., "Principles of Heat Transfer" 2nd ed. (International Textbook Co., Scranton, 1965).

7. Siegel, R. and Howell, J. R.: Thermal Radiation Heat Transfer. (McGraw Hill Co., New York, 1972), pp. 259-260.

8. Drummer, R. S. and Breckenridge, W. T., Jr., "Radiation Configuration Factors Program," ERR-AN-224, Feb. 1962, General Dynamics, San Diego, Calif.

9. Smith, J. P., "Systems Improved Numerical Differencing Analyzer (SINDA); User's Manual," TRW-14690-H001-R0-00, May 1971, TRW Systems Group, Redondo Beach, Calif.; also CR-134271, 1971, NASA.

TABLE I. - ASSUMED PHYSICAL PROPERTIES OF

ION THRUSTER MATERIALS

Material	ρ, g/cm^3	C_p, cal/(g)(°C) at 300° C	k, W/(cm)(°C) at 300° C
6061-T6 Al	2.77	0.20	1.80
Pure titanium	4.43	.15	.20
Carbon steel	7.81	.13	.60
304 Stainless	7.92	.125	.20
Molybdenum	10.19	.20	1.20
Tantalum	16.16	.035	.60
Mercury	13.56	.03	.10
Tungsten	19.38	.035	1.50
Alumina (Al_2O_3) (WESGO A1-300)	3.79	.20	.17
Kovar	8.36	.105	.15
6Al-4V titanium	4.43	.15	.10

TABLE II. - ASSUMED SELF HEATING POWER DISTRIBUTIONS

Component	J_B = 1 Amp		J_B = 1.9 Amps	
	Q, W	Percent Q	Q, W	Percent Q
Main vaporizer	7.3	3.46	7.3	2.13
Cathode vaporizer	4.6	2.17	7.6	2.21
Neutralizer tip	2.0	.96	3.4	.98
Neutralizer vaporizer	3.0	1.40	4.9	1.43
Cathode tip	13.4	7.26	25.6	7.43
Accelerator grid	11.6	5.52	19.6	5.68
Screen grid	11.6	5.52	19.6	5.68
Anode, rear	17.6	8.32	35.2	10.20
Anode, front	35.2	16.60	64.6	18.72
Engine body, rear	42.8	20.20	70.4	20.44
Engine body, front	9.2	4.44	15.6	4.52
Baseplate	36.8	17.32	46.8	13.60
Pole	14.4	6.84	24.0	6.96
TOTAL	209.5	100	344.4	100

Ion beam = 1 amp

Discharge power (arc) = 6.1 A x 37.2 V = 226 W

Ion beam = 1.9 amps

Discharge power (arc) = 10.1 A x 37.2 V = 376 W

TABLE III. - COMPARISON OF EXPERIMENTAL AND ANALYTICAL TEMPERATURES FOR CALIBRATION TESTS

Component	J_B = 1.9 Amps		J_B = 1.0 Amp	
	Experimental, °C	Analytical, °C	Experimental, °C	Analytical, °C
Main vaporizer	302	300	282	254
Baseplate	252	250	197	198
Engine body center				
Under neutralizer housing	204	208	149	153
90° from neutralizer	202	208	147	153
180° from neutralizer	205	207	150	152
270° from neutralizer	207	208	151	153
Engine body front				
Under neutralizer housing	253	261	182	197
90° from neutralizer	250	261	181	198
180° from neutralizer	262	261	191	197
270° from neutralizer	264	261	190	197
Anode, back	270	274	200	206
Rear shield[a]	141	141	106	106
Ground screen center				
90° from neutralizer	85	112	50	71
180° from neutralizer	84	112	51	71
270° from neutralizer	82	112	50	71

[a]Set to experimental value.

TABLE IV. - COMPARISON OF EXPERIMENTAL AND ANALYTICAL TEMPERATURE FOR MULTIPLE THRUSTER SIMULATION TESTS

Component \ Shield temperature, °C	J_B = 1.9 Amps				J_B = 1 Amp			
	30		150		-13		150	
	Experimental, °C	Analytical, °C	Experimental, °C	Analytical, °C	Experimental, °C	Analytical, °C	Experimental, °C	Analytical, °C
Main vaporizer	294	302	301	305	280	257	278	261
Baseplate	252	253	256	256	208	201	210	205
Engine body center								
Under neutralizer housing	207	201	209	206	161	148	163	155
90° from neutralizer	214	219	218	233	167	162	172	184
180° from neutralizer	221	219	224	234	174	162	178	185
270° from neutralizer	221	219	224	233	174	162	177	184
Engine body, front								
Under neutralizer housing	256	258	256	261	196	195	198	200
90° from neutralizer	258	262	259	269	198	199	203	210
180° from neutralizer	272	262	273	270	211	199	216	211
270° from neutralizer	272	262	273	269	209	199	213	210
Anode, back	270	276	274	279	215	208	217	213
Rear shield[a]	153	153	161	161	120	120	125	125
Ground screen center								
90° from neutralizer	132	127	141	155	95	84	104	124
180° from neutralizer	135	134	144	168	99	89	108	137
270° from neutralizer	132	127	140	155	95	84	104	124

[a]Set to experimental value.

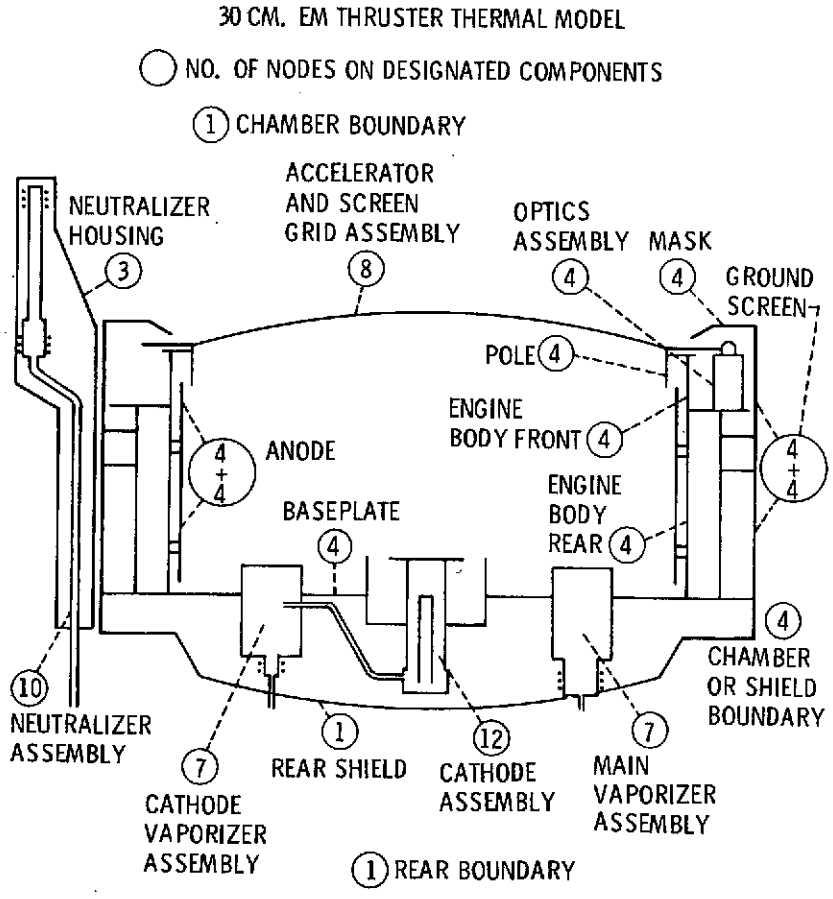

Figure 1. - Location of nodes in thermal model.

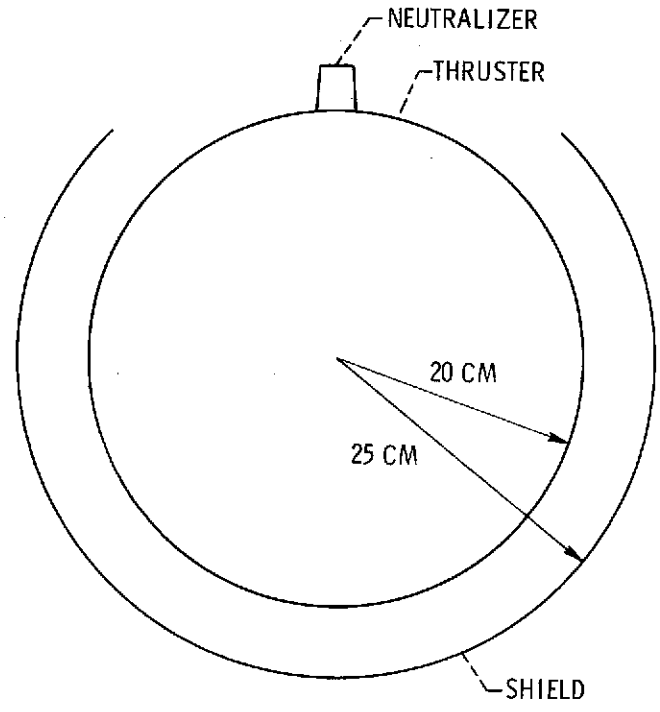

Figure 2. - Schematic of 30 centimeter ion thruster with 270^{0} axi muthal shield.

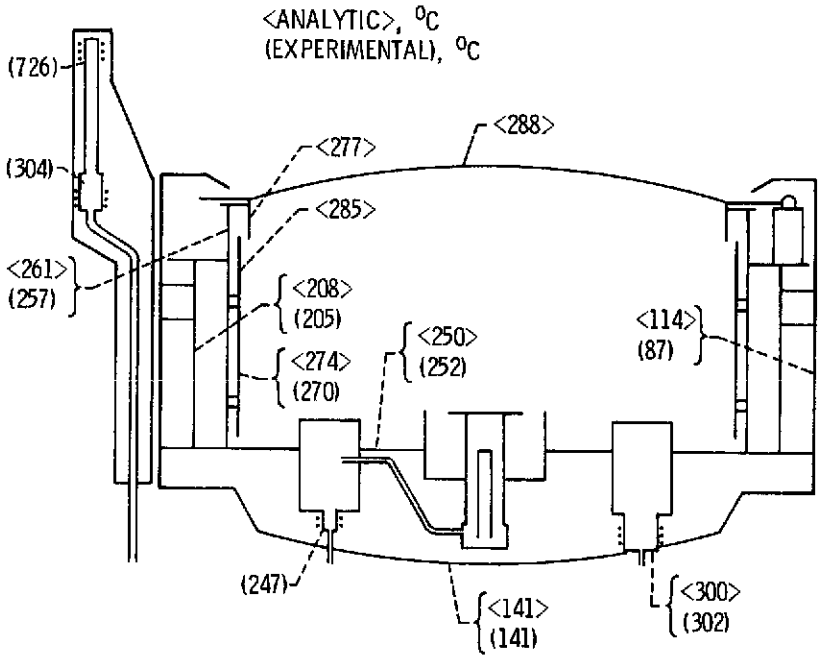

Figure 3. - Analytic and experimental results for a 1.9 amp beam current with no shield.

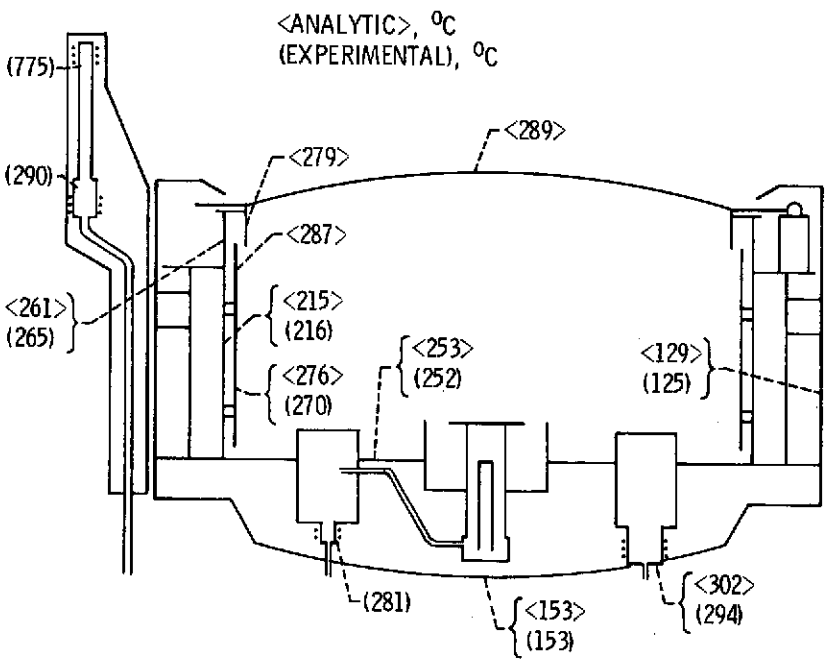

Figure 4. - Analytic and experimental results for a 1.9 amp beam current with the 270° azimuthal shield at 30° C.

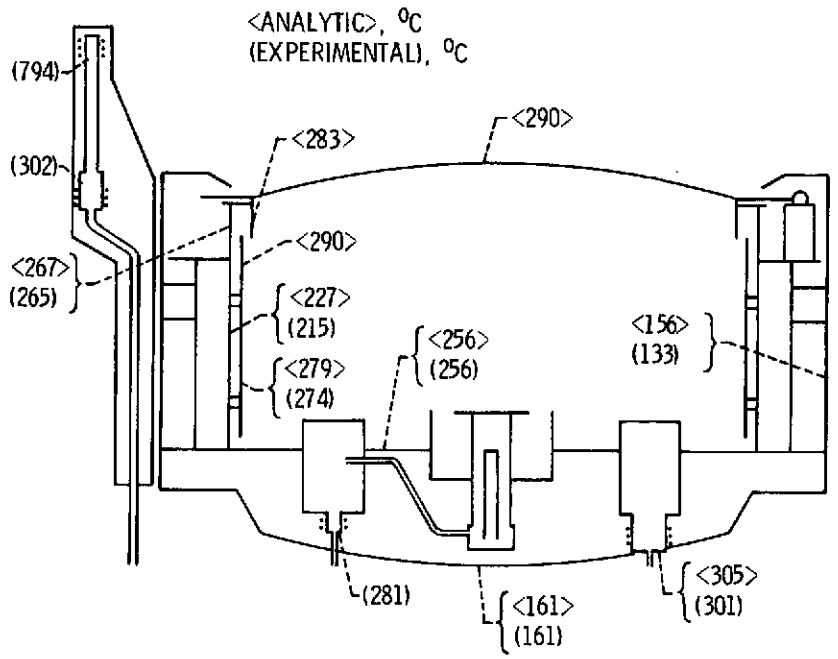

Figure 5. - Analytic and experimental results for a 1.9 amp beam current with the 270° azimuthal shield at 150° C.

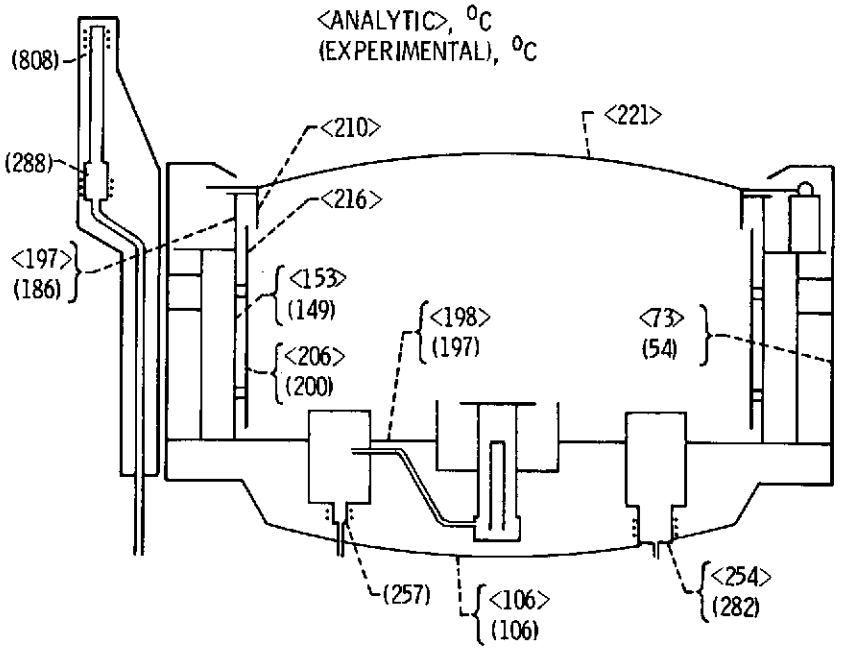

Figure 6. - Analytic and experimental results for a 1 amp beam current with no shield.

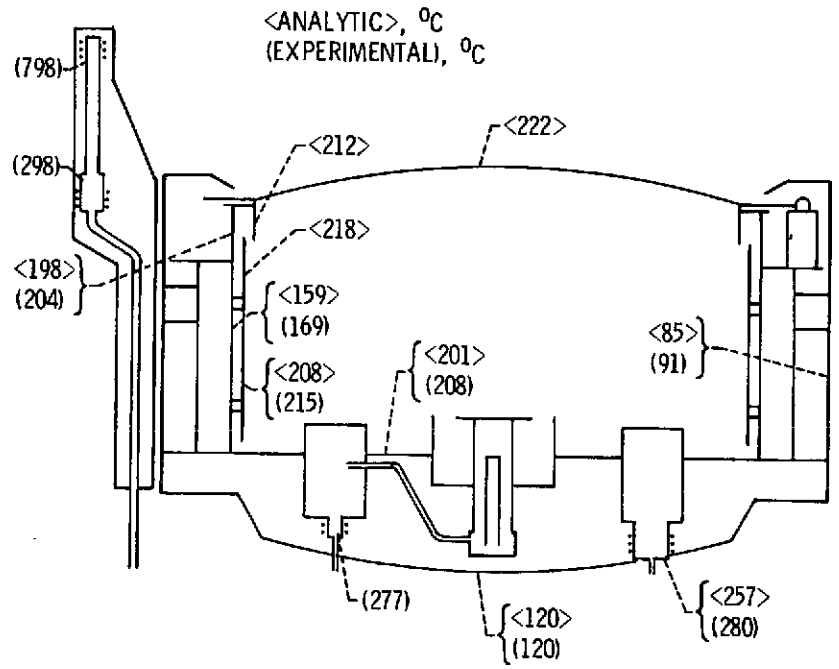

Figure 7. - Analytic and experimental results for a 1 amp beam current with the 270° azimuthal shield at -13° C.

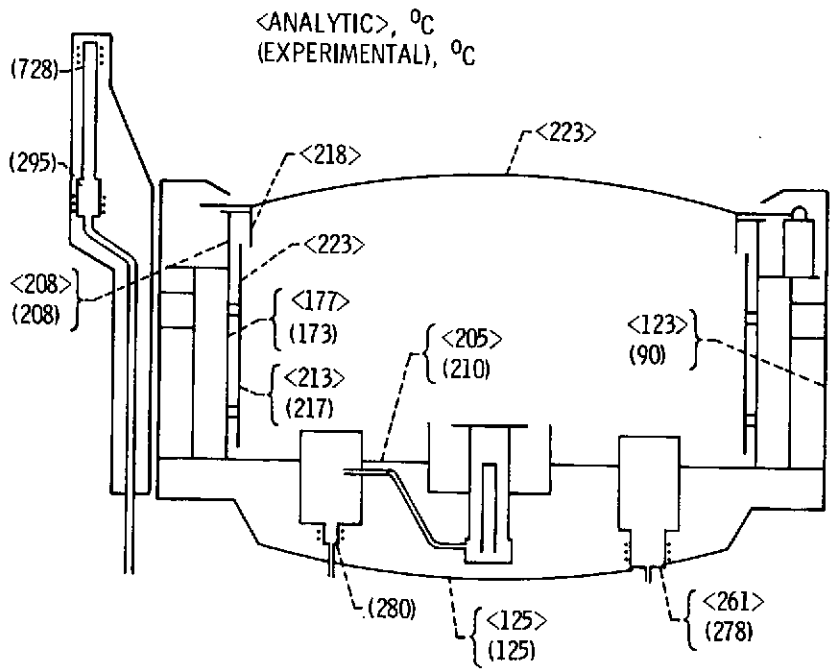

Figure 8. - Analytic and experimental results for a 1 amp beam current with the 270° azimuthal shield at 150° C.

NASA-Lewis